Regions of different critical behavior of the two-flavor Nambu–Jona-Lasinio model

Juan Xiong, Meng Jin, and Jiarong Li
Institute of Particle Physics, Huazhong Normal University, Wuhan 430079, China
(Received 12 October 2010; published 14 February 2011)

We study the chiral phase diagram in the T-μ-m_0 space of the two-flavor Nambu-Jona-Lasinio model with the approach of the Landau theory of phase transitions. The tricritical point (TCP) is an endpoint of a line of triple points as well as a crosspoint of three λ-transition lines. These double characters bring the connective and consistent problem of a critical phenomenon at the TCP. There is a crossover region from normal critical to tricritical behavior near the TCP, no matter whether the current quark mass is zero or not. The critical exponents need to be renormalized when one approaches the TCP along the first-order phase-transition line.

DOI: 10.1103/PhysRevC.83.025204 PACS number(s): 12.38.−t, 12.39.−x, 05.70.Jk

I. INTRODUCTION

The Lagrangian of quantum chromodynamics (QCD) has a marked character; i.e., it is chirally symmetric if the current quark mass is zero (chiral limit) while the chiral symmetry is explicitly broken if the current quark mass is nonvanishing. This dynamical character leads a series of thermodynamical properties of both QCD and the corresponding chiral model theories. Exploring the phase structure of QCD is one of the most exciting topics in the field of strong-interaction physics. In the temperature (T) and baryon chemical potential (μ_B) plane, recent lattice studies [1] and effective model studies [2] show that at sufficiently high μ_B, there is a first-order phase transition line between the chiral symmetry restored phase and broken phase. Moving along the phase boundary to higher T and lower μ_B, the first-order transition line ends in a TCP and becomes a second-order transition line for vanishing current quark mass, or it ends in a second-order critical point (critical endpoint CEP) and becomes a smooth crossover for nonzero current quark mass. The closer the current quark mass is to zero, the closer the CEP is to the TCP.

In statistical physics, the mechanism behind the occurrence of tricritical phenomena has been discussed qualitatively [3]. If a fictitious "field" h that is conjugate to the order parameter of the system exists, there will be two lines of critical endpoints emerging from the TCP symmetrically. Recently, Hatta [4] and Stephanov [5] gave some theoretical analyses of the symmetry group and universal class on the QCD phase diagram near the TCP. In the QCD theory, the current quark mass m_0 plays the role of external field h.

The critical phenomenon of the TCP is different from that of the CEP in principle. However, their critical regions may overlap if the current quark mass is small enough. Works [4,6] often discuss the critical region through calculating the ratio of baryon number susceptibility $\chi_B/\chi_B^{\mathrm{free}}$ and the theoretical basis that the TCP and CEP do not belong to the same universal class. Recently, the technique has been extended to study the sign of the third moments of conserved charges as well as their mixed moments [7]. Reference [4] pointed out that the hidden TCP can affect the critical phenomena around the CEP with nonzero current quark mass. However, a recent paper [8] with a nonlocal chiral model shows that there is no influence of the TCP properties on the CEP critical exponents. This indicates that whether the TCP affects the physics of CEP is an open problem. The critical point (CP) is the end of the two-phase coexistence line. The TCP is the endpoint of three-phase coexistence line. The CEP is the endpoint of two-phase coexistence line when the third phase still exists. We notice that these three points are relative as well as distinguishing, so in our paper we make an overall consideration in discussing the critical phenomena. We study the critical phenomena along different kinds of phase-transition lines, namely, the connection line of CEPs, the normal second-order phase-transition line, and the first-order phase-transition line.

One of the most thoroughly studied models in connection with the aspects of QCD chiral symmetry and its spontaneous breaking in the physical vacuum is the Nambu-Jona-Lasinio (NJL) model. The chiral transition line in the temperature and quark chemical potential plane calculated with the model is close to the result of a lattice QCD [9]. The two-flavor model Lagrangian takes the form [10]

$$\mathcal{L} = \bar{\psi}(i\gamma^\mu\partial_\mu - m_0 + \mu\gamma^0)\psi + G[(\bar{\psi}\psi)^2 + (\bar{\psi}i\gamma_5\tau\psi)^2]. \tag{1}$$

Here $\psi(\bar{\psi})$ is the quark (antiquark) field, m_0 is the current quark mass, and μ is the quark chemical potential. The interaction between quark fields is constructed in a manifestly chirally invariant fashion. Gluons do not appear explicitly but are subsumed in an effective contact interaction of strength G. In this paper, we will treat the NJL model in a mean-field theory by neglecting the fluctuation of the order parameter around its mean. At finite temperature, the NJL grand thermodynamical potential under the mean-field approximation can be determined as

$$\Omega(T,\mu;\sigma) = G\sigma^2 - 2N_cN_f\int_\Lambda \frac{d^3\vec{p}}{(2\pi)^3}E_p - 2N_cN_f\,T \int \frac{d^3\vec{p}}{(2\pi)^3}[\ln(1+\mathrm{e}^{-(E_p-\mu)/T}) + \ln(1+\mathrm{e}^{-(E_p+\mu)/T})], \tag{2}$$

where $E_p = \sqrt{\vec{p}^{\,2}+m_q^2}$ is the Hartree quasiparticle energy of the quark, and $m_q = m_0 - 2G\sigma$ is the constituent quark mass. The chiral-order parameter σ is defined as the condensation of quark-antiquark pairs, i.e., the vacuum expectation value $\langle\bar{\psi}\psi\rangle$. The three-dimensional momentum cutoff Λ is a regularization scheme in the NJL model. Its value depends on the detailed model parameters. $N_c(N_f)$ is the quark color (flavor) number.

II. THE TCP AND THE CONNECTION LINE OF CEPS

The Landau theory of phase transitions was developed by Landau in the 1940s, originally to describe superconductivity [11]. The procedure is general and is one of the most useful tools in condensed matter physics. The theory phenomenologically describes continuous phase transition using the change of thermodynamical potential and its relation with the order parameter at the phase transition point. It is a mean-field theory and emphasizes the importance of symmetry change in the phase transitions. The core of the theory grips the special property of system free energy, which contains a surprising amount of information about the physics of phase transitions.

In this section, we start from the Landau theory of phase transitions and study a T-μ-m_0 phase diagram of the two-flavor NJL model. In the vicinity of the critical point, the order parameter σ is an arbitrary small quantity. We expand the grand thermodynamical potential to the sixth power of chiral-order parameter σ and omit the third and fifth power terms. The Landau function has the following form:

$$\Omega(T,\mu;\sigma) = \tfrac{1}{2}a\sigma^2 + \tfrac{1}{4}b\sigma^4 + \tfrac{1}{6}c\sigma^6 - h\sigma. \quad (3)$$

The coefficients a, b, c, h of the Landau expansion are functions of (T,μ). Their explicit expressions are given in the Appendix. With the detailed model parameters [12], we could obtain numerical results. Here h is an external field that couples directly to the order parameter σ. One has

$$h = -\frac{\partial\Omega}{\partial\sigma}. \quad (4)$$

In the NJL model the current quark mass m_0 plays the role of h. From Eq. (A2) we know that when $m_0 = 0$, h equals zero.

Figure 1 shows a chiral phase diagram of the two-flavor NJL model in the T-μ-m_0 space. We display analytical expressions of four curves connected with the TCP in the following. The

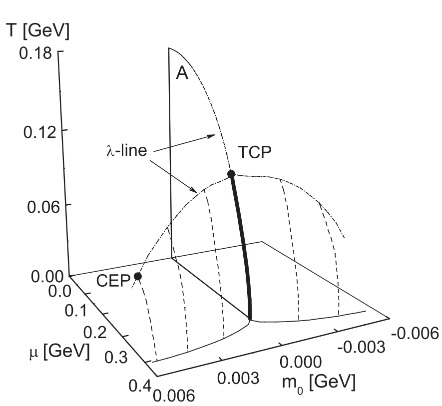

FIG. 1. Chiral phase diagram in T-μ-m_0 space of the two-flavor NJL model.

λ-line (three dash-dotted lines) is given in general form by

$$\frac{\partial^2\Omega}{\partial\sigma^2} = \frac{\partial^3\Omega}{\partial\sigma^3} = 0. \quad (5)$$

With the Landau free energy (3) and field h's expression (4), Eqs. (5) yield

$$a = 0, \quad h = 0, \quad (6)$$

and in addition

$$a = \frac{9b^2}{20c}, \quad h = \pm\frac{8c}{3}\left(\frac{-3b}{10c}\right)^{\frac{5}{2}}. \quad (7)$$

Substituting the expansive coefficients in the Appendix into Eq. (6), and noticing that $b > 0$, Eq. (6) gives the relation between T and μ through the T- and μ-dependent coefficients a and h, which is shown by the dash-dotted line in $m_0 = 0$ ($h = 0$) plane. Similarly, Eq. (7) determines the other two λ lines for nonzero quark mass, which will be discussed later. In the Landau theory of phase transitions, the three λ lines are of the normal second-order phase-transition line. The Landau theory also predicts a first-order phase-transition line (τ line) in the $m_0 = 0$ plane. When we neglect the linear term, the Landau expansion formula [Eq. (3)] becomes a typical ϕ^6 potential, which has one minimum at $\sigma = 0$ and two other symmetric minima. At critical T and μ of the first-order phase transition, the values of three local minima of $\Omega(T,\mu;\sigma)$ are equal. The analytical equations determining the first-order phase transition line are

$$b^2 = \tfrac{16}{3}ac, \quad b < 0, \quad h = 0. \quad (8)$$

The numerical result is shown by the thick solid line in Fig. 1. We notice that it connects with three λ lines at the TCP. At the TCP, $a = b = 0$, and the three-local-minimum structure of $\Omega(T,\mu;\sigma)$ vanishes.

In the $m_0 = 0$ plane, one has a first-order coexistence surface A. On the two sides of the A plane, the order parameter undertakes nonzero values with opposite signs depending on whether $m_0 \to 0$ from positive or negative directions. (This is a theoretical analysis. Actually, m_0 must be positive in the real world.) As T increases, the surface A terminates in a line of critical points, the λ line (the dash-dotted line in $m_0 = 0$ plane), and for $T < T^{\mathrm{TCP}}$, it terminates in the two-phase coexistence curve (τ line). From Fig. 1 one notes that through the τ line, A is connected to two first-order surfaces (the wings) extending symmetrically into the regions of $m_0 > 0$ and $m_0 < 0$, respectively. The wings themselves terminate with increasing temperature in two lines of CEPs (the two dash-dotted lines in space). These two lines of CEPs also indicate the λ transition given by Eq. (7). The three λ lines join together at the TCP. Therefore, the TCP may be regarded either as the termination of a line (τ line of $m_0 = 0$) of triple points or, equivalently, as the confluence of three λ lines. With our model parameters, the TCP is located at $T^{\mathrm{TCP}} = 0.1$ GeV and $\mu^{\mathrm{TCP}} = 0.267$ GeV.

The dashed curves on the surface of the wing in Fig. 1 indicate the first-order coexistence curves at different quark current mass m_0. The end of each line is a CEP. In order to highlight the meaning of CEP, we confine ourselves to $m_0 = 0.0055$ GeV and elaborate how to fix the corresponding

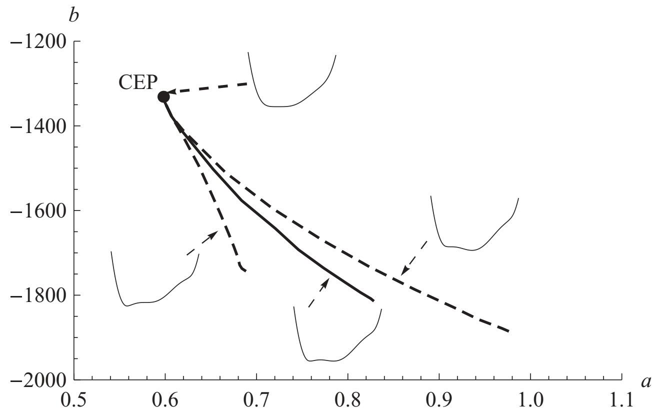

FIG. 2. Phase diagram on the a-b plane at $m_0 = 0.0055$ GeV of the two-flavor NJL model. The thin solid curves indicate different types of the grand thermodynamical potential as functions of order parameter σ.

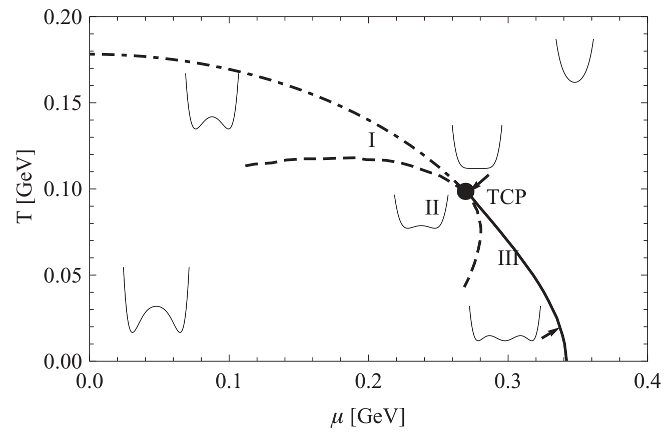

FIG. 3. The chiral phase diagram in the $m_0 = 0$ plane of the two-flavor NJL model. Indices I, II, and III indicate the regions of different critical behavior in the chiral symmetry broken phase. The thin curves indicate different types of the grand thermodynamical potential as functions of order parameter σ.

first-order phase transition line and the CEP. The thick solid line in Fig. 2 represents the first-order coexistence curve. The thin solid curves indicate different types of the grand thermodynamical potential as functions of order parameter σ. Since $h \neq 0$, the linear term in the ϕ^6 potential exists. So the $\Omega(T,\mu;\sigma)$ exists three minima that are not symmetric about $\sigma = 0$. In the three minima, one is higher and always exists at any T,μ. The other two are lower. The first-order coexistence curve is determined by the critical T,μ when the other two local minima of $\Omega(T,\mu;\sigma)$ are equal. At the CEP, the two-local-minimum structure vanishes while the third local minimum still exists. With explicit model parameters, we obtain the detailed axis values in the a-b plane. (The two dashed curves in Fig. 2 represent two metastable states.) From this discussion we can see that (1) three coexisting and distinct phases become identical simultaneously at a TCP; (2) if two phases become identical in the presence of a third phase, which remains distinct, that thermodynamic state is called a CEP; and (3) two phases become identical at an ordinary CP. We reiterate these concepts in order to stress that their properties would result in a deeper understanding of the critical phenomena, which we will discuss in the following.

III. REGIONS OF DIFFERENT CRITICAL BEHAVIOR

First, we discuss the situation at the chiral limit. Figure 3 shows the T-μ phase diagram. In the $m_0 = 0$ plane the second-order phase transition line (λ line) meets the first-order phase-transition line (τ line) at the TCP. The dash-dotted line indicates the λ transition, and the heavy solid line indicates the τ transition.

In Fig. 3 the thin solid curves show the shapes of the grand thermodynamical potential for the chiral-order parameter σ. In the chiral symmetry broken phase, the potential has two equal minima. On the τ line, the potential has three equal minima that fuse into one minimum at the TCP as discussed in Sec. II. In the region near the TCP, we could not observe a distinct difference of the grand thermodynamical potential. In the chiral symmetry restored phase, the potential has only one minimum. The Landau theory predicts a uniform set of critical exponents. In the chiral symmetry broken phase, all critical exponents are determined by the value of the order parameter and need to be discussed in different regions. With thermodynamical conditions

$$\frac{\partial \Omega}{\partial \sigma} = 0, \ \frac{\partial^2 \Omega}{\partial \sigma^2} > 0, \tag{9}$$

and for $m_0 = 0$, we have

$$\sigma_0^2 = \frac{-b + \sqrt{b^2 - 4ac}}{2c}. \tag{10}$$

This allows us to analyze the critical behavior in different regions. In region I, defined by $b^2 \gg -4ac$, we retain the linear term, and Eq. (10) gives approximately

$$\sigma_0^2 \approx -\frac{a}{b}. \tag{11}$$

We assume that the slope of the λ line at the TCP is finite; then Eq. (11) yields a normal critical exponent. This is a typical ϕ^4 theory of phase transitions. We calculate the critical exponent β_λ as an example. One assumes that $a = a_0 t (a_0 > 0)$ and b is a positive constant, and t is the reduced temperature $\frac{T - T_\lambda}{T_\lambda}$, with T_λ the critical temperature of the phase transition. We start from the definition $\sigma \sim |t|^\beta$. Substituting Eq. (11), one has $\sigma_0 \approx \pm\sqrt{\frac{a_0}{b}}|t|^{\frac{1}{2}}$. Thus the critical exponent $\beta_\lambda = \frac{1}{2}$. In region II, defined by $b^2 \ll -4ac$, one has

$$\sigma_0^2 \approx \sqrt{-\frac{a}{c}}. \tag{12}$$

Equation (12) yields a normal tricritical exponent $\beta_t = \frac{1}{4}$. This is a typical critical exponent of the phase transition theory of ϕ^6. Region III is the other part of the vicinity of the TCP excluding the region I and II in the chiral symmetry broken phase.

Based on this discussion, one obtains that when $b^2 \sim -4ac$ there is a region in which the types of critical exponents transfer from ϕ^4 to ϕ^6. In Fig. 4 we show a numerical result of the phase diagram on the a-b plane at the chiral limit. The dash-dotted

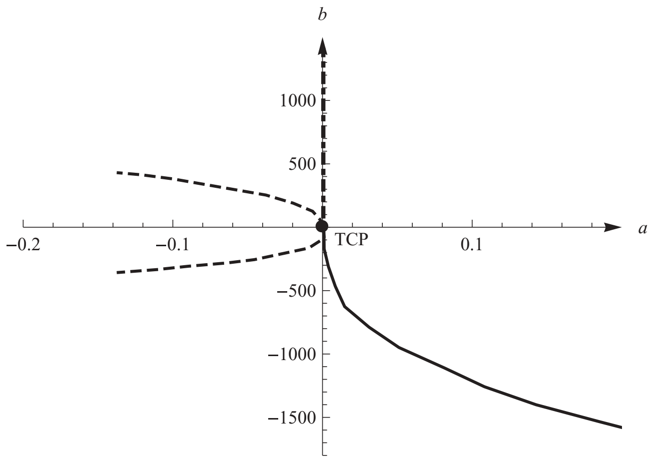

FIG. 4. The crossover regions of critical behavior from ϕ^4 to ϕ^6 on the a-b plane at the chiral limit of the two-flavor NJL model.

line displays the normal second-order phase transition. The black solid curve is of a first-order phase-transition whose analytical expression is as shown as Eq. (8). The dashed curve corresponds to $b^2 = -4ac$. For $b > 0$, the region around the dashed curve has critical exponents lying between normal critical and tricritical exponents. This region is termed the ϕ^4-ϕ^6 crossover region. The ratio of $\frac{b^2}{4a_0c}$ is a proper indicator characterizing the normal critical to tricritical crossover behavior. Its magnitude decides how close the thermodynamical system is to the TCP and whether the crossover behavior can be observed. As the TCP is approached, the range of the normal critical behavior region decreases and shrinks to zero at the TCP. We calculate the temperature T_0 and quark chemical potential μ_0 that satisfy the equation $b^2 = -4ac$. According to our numerical results, $|T_0 - T^{\mathrm{TCP}}|$, $|\mu_0 - \mu^{\mathrm{TCP}}|$ are within the limit of 5 MeV.

Second, we turn to the $m_0 \neq 0$ situation. One approaches the TCP along the connection line of the CEPs, i.e., the other two λ lines in space in Fig. 1, and discusses the corresponding critical behavior. From the viewpoint of theoretical unification, we should do some analysis as follows for the $m_0 \neq 0$ case: Step 1: Find the analytical solution σ_m of

$$\frac{\partial\left(\frac{1}{2}a\sigma^2 + \frac{1}{4}b\sigma^4 + \frac{1}{6}c\sigma^6 - h\sigma\right)}{\partial\sigma} = 0.$$

Step 2: According to the character of σ_m explore possible critical regions in the vicinity of the CEP, such as the approach of the $m_0 = 0$ situation with Eqs. (10)–(12). However, the general solution of a quintic in terms of generalized hypergeometric functions is of little help in analyzing the regions of different critical behaviors. On the other hand, as is well known, the critical exponents determine the behavior of relevant thermodynamical quantities in the vicinity of the second-order phase transition line. We specially calculate the quark number susceptibility χ at the CEP with the path parallel to the μ axis in the T-μ plane. The quark number susceptibility χ is defined by

$$\chi = -\frac{\partial^2\Omega}{\partial\mu^2}. \tag{13}$$

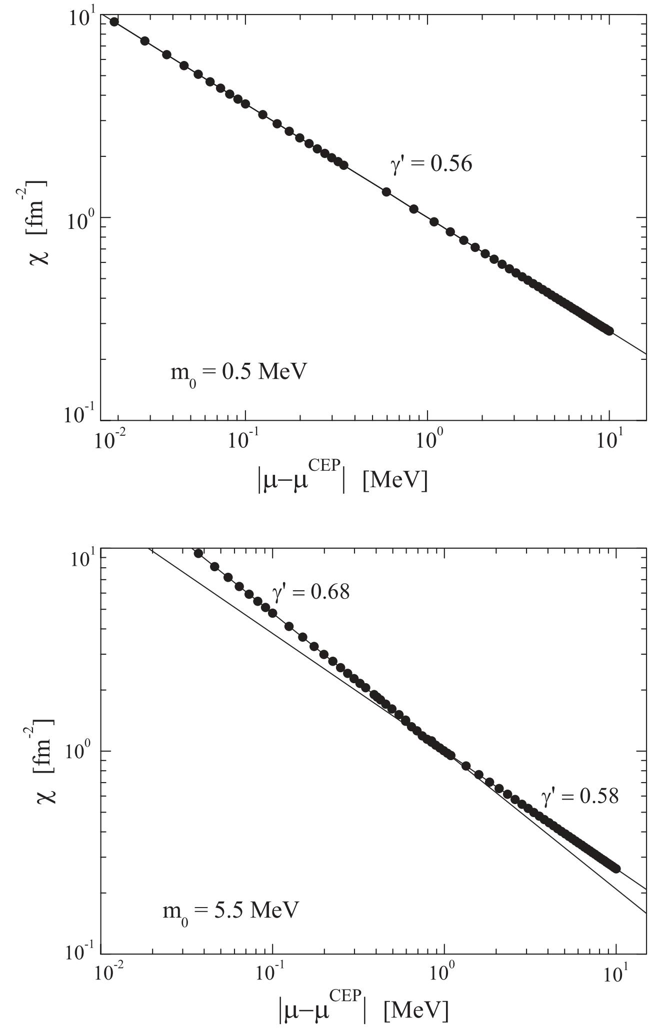

FIG. 5. The quark number susceptibility for $m_0 = 0.5$ MeV (upper panel) and 5.5 MeV (lower panel) as functions of $|\mu - \mu^{\mathrm{CEP}}|$ at corresponding critical quark chemical potential $\mu^{\mathrm{CEP}}(m_0)$.

Following the general definition of critical exponent, we use a linear logarithmic fit

$$\ln\chi = -\gamma'\ln|\mu - \mu^{\mathrm{CEP}}|, \tag{14}$$

where $|\mu - \mu^{\mathrm{CEP}}|$ is the distance to the CEP and γ' is critical exponent. In Fig. 5, χ is plotted for $m_0 = 0.5$ MeV (upper panel) and $m_0 = 5.5$ MeV (lower panel). For $m_0 = 0.5$ MeV situation, we obtain $\gamma' = 0.56$. Compared to the normal critical mean field theory $\frac{2}{3}$, it is closer to the mean-field value of TCP $\frac{1}{2}$. At $m_0 = 5.5$ MeV, we obtain $\gamma' = 0.68$ in the $|\mu - \mu^{\mathrm{CEP}}| < 0.5$ MeV region and $\gamma' = 0.58$ in the $|\mu - \mu^{\mathrm{CEP}}| > 1$ MeV region, respectively. According to the changing behavior of the critical exponent, when one approaches the TCP along the line of CEPs, there also exists a crossover region. This result is in agreement with Ref. [4]. To recognize how strong is the suppression of the effect of the hidden TCP with increasing m_0, we increase the current quark mass m_0 to 7 MeV and calculate the critical exponent of the quark number susceptibility. The result indicates that the effect of the hidden TCP vanishes until this point. Our study is helpful in the understanding of the connection and difference of the CEP, TCP, and CP.

IV. RENORMALIZATION OF THE CRITICAL EXPONENT IN THE FIRST-ORDER PHASE-TRANSITION REGION

Since the TCP is a connection point of the λ line and τ line, how do the critical phenomena become consistently and continuously at this point if we are approaching it along the λ line and τ line, respectively? We turn to studying the property of the response function. The quark number susceptibilities χ as a function of the temperature T for three different values of quark chemical potential μ are displayed in Fig. 6. The susceptibility χ diverges at the TCP. We take a normalized scale factor C to make it finite in order to compare χ at different situations. For quark chemical potential μ below μ^{TCP}, in the second-order phase-transition region, the response function displays a narrow peak. which is shown as the dotted curve. For $\mu = \mu^{\mathrm{TCP}}$, the χ/C indicates a sharper and narrower peak at the transition temperature (as shown as the dashed-dotted curve) than in the second-order phase-transition case. These two behaviors show a consistent and continuable trend in the way of approaching the TCP along the λ line. Now we turn to the discussion along the τ line. For chemical potential above μ^{TCP}, we have a first-order phase transition, and, consequently, χ/C has a discontinuity. It rises straight up to positive infinity and drops down to negative infinity immediately and then finally jumps back to zero. Literature often show a broken and discontinued behavior of the response function in the first-order phase-transition region.

In region III of Fig. 3, we care about the critical phenomena in the vicinity of the TCP along the first-order phase-transition line. Since it is usually rather hard to know whether the thermodynamical function really diverges to infinity or whether it has only a sharp but finite cusp at critical temperature, the corresponding critical exponents are less well determined. We notice that boundaries of region III and the λ line have the same slope at the TCP. This means the behavior of χ/C should be a finite cusp instead of diverge when approaching the TCP in region III. Fisher [13] pointed out that for any system that can display a divergent specific-heat anomaly there will be natural circumstances in which the system will be characterized by renormalized critical exponents and a finite, although sharply cusped, finite specific heat. He also discussed a variety of exactly soluble models where this renormalization can be checked explicitly. In condensed matter physics, this theory has been widely applied [14]. Following this idea, when approaching the TCP along the τ line, the tricritical exponents are needed for renormalization. They are given by

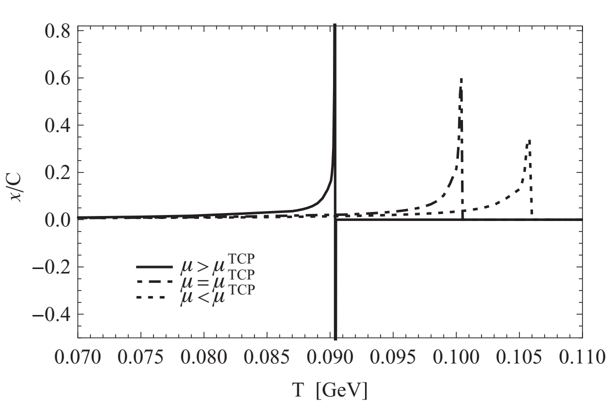

FIG. 6. Behavior of the scaled quark number susceptibility χ/C as functions of temperature T at three values of quark chemical potential.

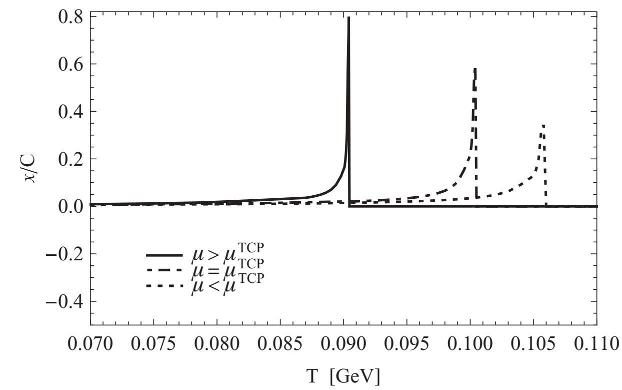

FIG. 7. Behavior of the scaled quark number susceptibility χ/C as functions of temperature T. The critical exponent is renormalized in the case of $\mu > \mu^{\mathrm{TCP}}$.

$$\begin{aligned}
\alpha_\tau^- &= -\alpha_t/(1-\alpha_t),\\
\beta_\tau^- &= \beta_t/(1-\alpha_t),\\
\gamma_\tau^- &= \gamma_t/(1-\alpha_t),\\
\nu_\tau^- &= \nu_t/(1-\alpha_t).
\end{aligned} \tag{15}$$

The subscript t represents the critical exponents of the mean field at the TCP. Then the renormalized tricritical exponents arising are the following: $\alpha_\tau^- = -1$, $\beta_\tau^- = \frac{1}{2}$, $\gamma_\tau^- = 2$, $\nu_\tau^- = 1$. The superscript $-$ means to approach the transition point from the chiral symmetry broken phase. These renormalized exponents also satisfy the same homogeneity or scaling relations [13]. For example, $\alpha_\tau^- + 2\beta_\tau^- + \gamma_\tau^- = 2$.

We calculate the scaled susceptibility χ/C after renormalization and show the numerical results in Fig. 7. When $\mu > \mu^{\mathrm{TCP}}$, χ/C shows a cusplike type approaching the critical point. So this behavior is consistent and continuable with the transition at the TCP and along the λ line.

In the current quark mass m_0 nonzero situation, there also exists a connecting point, the CEP, joining the first-order chiral phase-transition line and crossover transition line together. We know the chiral phase transition at the CEP itself is of second order. So in the nonzero m_0 plane, the critical exponents of the CEP also need to be renormalized when approaching it along the direction of the τ-transition line (the dashed curve on the surface of the wing in Fig. 1).

V. SUMMARY AND DISCUSSION

Through the Landau theory of phase transitions, we represent a T-μ-m_0 chiral phase diagram of the two-flavor

NJL model under the mean-field approximation. We explicitly reveal the relation of TCP, CEP, and CP. We also emphasize a few issues that should be noted in discussing the critical behavior of the NJL model. Namely, in the T-μ plane of $m_0 = 0$, one should study along both the λ-line and τ-line to approach the TCP. On the other hand, in the T-μ-m_0 figure of the $m_0 \neq 0$ situation, one should study along the connection line of CEPs to approach the TCP.

Our results are the following. First, the critical behavior of the λ line that is follows the ϕ^6 theory could not simply be recognized as the same as that of the second-order phase-transition line following the ϕ^4 theory. There is a crossover region of the critical behavior when one approaches the TCP from different directions in the T-μ-m_0 space. Second, when m_0 is very small, the hidden TCP would affect the critical behavior near the CEP. Third, when approaching the TCP along τ line, one should adopt the renormalized critical exponents that were created by Fisher. Finally, we expect that our conclusion could be helpful for high-energy ion experiments in exploring the phase boundary and the CEP location through energy scanning.

Condensed matter physics has long been concerned about the CEP (CP) behavior near and away from the TCP. Reference [15] pointed out that there may be crossover regions from the CEP (CP) to the TCP. In high-energy physics, Ref. [4] first discussed the issue that the TCP may affect the physics near the CEP and indicated a crossover of different university classes by using a Cornwall-Jackiw-Tomboulis effective potential for the two-flavor QCD. Our paper extends their work. The results show that there exist crossover regions from either the CP or the CEP approaching the TCP. Renormalization of critical exponents is also a well-studied problem in condensed matter physics. We try to apply the idea to the NJL model. We discuss the qualitatively consistent problem of the critical exponents when one approaches the TCP from the first-order phase-transition line. However, the factor or mechanism that results in the renormalization also requires in-depth analysis.

ACKNOWLEDGEMENT

The work is supported by NSFC Grants 10805023, 10875050, and 10675052.

APPENDIX

At the chiral limit $m_0 = 0$, the explicit expressions of the coefficients in Eq. (3) are

$$
\begin{aligned}
\frac{1}{2}a(T,\mu) &= G - \frac{12G^2}{\pi^2}\int_0^{\Lambda} k\,dk + \frac{12G^2}{\pi^2}\int k[f(k+\mu)+f(k-\mu)]\,dk,\\
\frac{1}{4}b(T,\mu) &= \frac{12G^4}{\pi^2}\int_0^{\Lambda}\frac{1}{k}\,dk - \frac{12G^4}{\pi^2}\int\left\{\frac{1}{T}[f(k+\mu)+f(k-\mu)-f^2(k+\mu)-f^2(k-\mu)]\right.\\
&\quad\left. + \frac{1}{k}[f(k+\mu)+(f(k-\mu)]\right\}dk,\\
\frac{1}{6}c(T,\mu) &= -\frac{48G^6}{\pi^2}\int_0^{\Lambda}\frac{1}{k^3}\,dk + \frac{16G^6}{\pi^2}\int 3\left(\frac{1}{3T^2k}+\frac{1}{k^2T}+\frac{1}{k^3}\right)[f(k+\mu)+f(k-\mu)]\\
&\quad - \left(\frac{1}{T^2k}+\frac{1}{k^2T}\right)[f^2(k+\mu)+f^2(k-\mu)] + \frac{2}{T^2k}[f^3(k+\mu)+f^3(k-\mu)]\,dk.
\end{aligned} \tag{A1}
$$

Here $f(k \pm \mu)$ is the Fermi-Dirac distribution $f(k\pm\mu) = \frac{1}{1+e^{\frac{k\pm\mu}{T}}}$. At the real-world $m_0 \neq 0$ situation, we enumerate the coefficients of linear and quadric terms of the Landau expansion. About the coefficients of fourth and sixth power terms, since the calculation is similar and the expressions are trite, we do not show the expressions here.

$$
\begin{aligned}
h(T,\mu;m_0) &= \frac{12Gm_0}{\pi^2}\int_0^{\Lambda}\frac{k^2}{E_k}\,dk - \frac{12Gm_0}{\pi^2}\int\frac{k^2}{E_k}[f(k+\mu)+f(k-\mu)]\,dk,\\
\frac{1}{2}a(T,\mu;m_0) &= G - \frac{12G^2}{\pi^2}\int_0^{\Lambda}\frac{k^4}{E_k^3}\,dk + \frac{12G^2}{\pi^2}\int k^2\left\{\frac{m_0^2}{TE_k^2}[f^2(E_k+\mu)+f^2(E_k-\mu)]\right.\\
&\quad\left. - \frac{1}{E_k}\left(\frac{m_0^2}{TE_k}+\frac{m_0^2}{E_k^2}-1\right)[f(E_k+\mu)+f(E_k-\mu)]\right\}dk,
\end{aligned} \tag{A2}
$$

where $E_k = \sqrt{k^2+m_0^2}$.

[1] Z. Fodor and S. Katz, J. High Energy Phys. 03 (2002) 014; P. de Forcrand and O. Phillipsen, Nucl. Phys. B **642**, 290 (2002); M. D'Elia and M. P. Lombardo, Phys. Rev. D **67**, 014505 (2003); C. R. Allton *et al.*, *ibid.* **66**, 074507 (2002); C. R. Allton, S. Ejiri, S. J. Hands, O. Kaczmarek, F. Karsch, E. Laermann, and C. Schmidt, *ibid.* **68**, 014507 (2003).

[2] M. Alford, K. Rajagopal, and F. Wilczek, Phys. Lett. B **422**, 247 (1998); R. Rapp, T. Schafer, E. V. Shuryak, and M. Velkovsky, Annals Phys. **280**, 35 (2000); J. Berges and K. Rajagopal, Nucl. Phys. B **538**, 215 (1999); O. Scavenius, A. Mocsy, I. N. Mishustin, and D. H. Rischke, Phys. Rev. C **64**, 045202 (2001).

[3] S. Dattagupta, Bull. Mater. Sci. **3**, 133 (1981).

[4] Y. Hatta and T. Ikeda, Phys. Rev. D **67**, 014028 (2003).

[5] M. Stephanov, Prog. Theor. Phys. Suppl. **153**, 139 (2004).

[6] P. Costa, M. C. Ruivo, and C. A. de Sousa, Phys. Rev. D **77**, 096001 (2008); P. Costa, C. A. de Sousa, M. C. Ruivo and Yu. L. Kalinosky, Phys. Lett. B **647**, 431 (2007); C. A. de Sousa, P. Costa, and M. C. Ruivo, Frascati Phys. Ser. **46**, 767 (2007); P. Costa, C. A. de Sousa, M. C. Ruivo, and H. Hansen, Europhys. Lett. **86**, 31001 (2009).

[7] M. Asakawa, S. Ejiri, and M. Kitazawa, Phys. Rev. Lett. **103**, 262301 (2009).

[8] G. A. Contrera, M. Orsaria, and N. N. Scoccola, Phys. Rev. D **82**, 054026 (2010).

[9] U. Vogl and Weise, Prog. Part. Nucl. Phys. **27**, 195 (1991); S. P. Klevansky, Rev. Mod. Phys. **64**, 649 (1992); T. Hatsuda and T. Kunihiro, Phys. Rep. **247**, 221 (1994); J. Hufner, S. P. Klevansky, P. Zhuang, and H. Voss, Ann. Phys. (NY) **234**, 225 (1994); P. Zhuang, M. Huang, and Z. Yang, Phys. Rev. C **62**, 054901 (2000).

[10] P. F. Zhuang, J. Hufner, and S. P. Klevansky, Nucl. Phys. A **576**, 525 (1994).

[11] L. D. Landau and E. M. Lifshitz, *Statistical Physics*, 3rd Edition (World Book Publishing Company, Singapore, 2007).

[12] K. Kashiwa, H. Kouno, M. Matsuzaki, and M. Yahiro, Phys. Lett. B **662**, 26 (2008); J. Xiong, M. Jin, and J. Li, J. Phys. G: Nucl. Part. Phys. **36**, 125005 (2009).

[13] M. E. Fisher, Phys. Rev. **176**, 257 (1968).

[14] M. E. Fisher, Rev. Mod. Phys. **70**, 653 (1998); Y. Achiam and Y. Imry, J. Phys. C **10**, 39 (1977); R. Bausch, Z. Phys. **254**, 81 (1972); I. M. Mryglod, I. P. Omelyan, and R. Folk, Phys. Rev. Lett. **86**, 3156 (2001); D. A. Huse, *ibid.* **55**, 2228 (1985).

[15] R. Shashidhar, B. R. Ratna, G. G. Nair, S. K. Prasad, Ch. Bahr, and G. Heppke, Phys. Rev. Lett. **61**, 547 (1988); B. R. Ratna, R. Shashidhar, G. G. Nair, S. K. Prasad, C. Bahr, and G. Heppke, Phys. Rev. A **37**, 1824 (1988); C. C. Huang and J. M. Viner, *ibid.* **25**, 3385 (1982); A. Kumar, Physica A **146**, 634 (1987).